MOLECULAR AND CELLULAR BIOLOGY, Aug. 2000, p. 5777–5787 Vol. 20, No. 15
0270-7306/00/$04.00+0

Architecture of the Replication Fork Stalled at the 3′ End of Yeast Ribosomal Genes

MARKUS GRUBER, RALF ERIK WELLINGER, AND JOSÉ M. SOGO*

Institute of Cell Biology, ETH Hönggerberg, CH-8093 Zürich, Switzerland

Received 8 February 2000/Returned for modification 22 March 2000/Accepted 25 April 2000

Every unit of the rRNA gene cluster of *Saccharomyces cerevisiae* contains a unique site, termed the replication fork barrier (RFB), where progressing replication forks are stalled in a polar manner. In this work, we determined the positions of the nascent strands at the RFB at nucleotide resolution. Within an *Hpa*I-*Hin*dIII fragment essential for the RFB, a major and two closely spaced minor arrest sites were found. In the majority of molecules, the stalled lagging strand was completely processed and the discontinuously synthesized nascent lagging strand was extended three bases farther than the continuously synthesized leading strand. A model explaining these findings is presented. Our analysis included for the first time the use of T4 endonuclease VII, an enzyme recognizing branched DNA molecules. This enzyme cleaved predominantly in the newly synthesized homologous arms, thereby specifically releasing the leading arm.

DNA replication is a complex process that can be divided into three steps: initiation, ongoing replication, and termination. Whereas extensive work has been done on the first of these steps, only little is known about the last, even though hundreds of termination events occur every time the genome of an eukaryotic organism is replicated. Replication termination in the chromosomes of *Saccharomyces cerevisiae* seems to occur throughout a broad region, whenever two converging replication forks meet, rather than at specific sites (4, 30). An exception to this rule is represented by the specific replication termination site at the 3′ end of the rRNA transcription unit, the replication fork barrier (RFB). The RFB was originally found in the yeast *S. cerevisiae* (5, 22) and subsequently observed in many disparate organisms including *Schizosaccharomyces pombe*, frog, mouse, human, and plant (12, 13, 23, 24, 36, 45). Thus, the RFB seems to be a common feature of eukaryotic rDNA replication (13). The location of the stalled fork at the RFB in *S. cerevisiae* was narrowed down to a 129-bp restriction fragment defined by a *Hin*dIII-*Hpa*I restriction site (Fig. 1; see also reference 6). Furthermore, the sequences required for the block seem to reside within this fragment, even though additional sequences could be necessary to restore the full functionality of the RFB (6, 19).

The molecular mechanism of the RFB, however, remains elusive. It has been demonstrated that transcription elongation is not a prerequisite for a functional RFB, since the blockage was observed in a strain lacking RNA polymerase I (6). However, in this yeast strain even nucleosome-free enhancers have been detected which can have RFB activity (9). Moreover, sequences close to the 3′ end of the 35S rRNA gene (rDNA) retained their blocking ability when inserted into extrachromosomal plasmids lacking the transcription unit (6, 19). On the other hand, these sequences did not impede replication fork movement on a plasmid in *Escherichia coli*, excluding possible structures inherent in the DNA sequence. This finding led to the suggestion that a specific protein binds to the RFB sequence, impeding the movement of the replication fork (6).

An attractive candidate for such a protein has been reported by Kobayashi and Horiuchi (20). Mutations in a protein termed Fob1 were shown to be responsible for HOT1 (hot spot of recombination) and RFB defects (20). In this context it is noteworthy that *fob1* mutants, in which replication of the rDNA is bidirectional, do not show any obvious growth defects (20). Further investigations have revealed that Fob1 is involved in the expansion and contraction of the rDNA repeats (18). The elimination of Fob1 extends the life span of yeast mother cells by slowing down the generation of circular extrachromosomal rDNA circles (ERCs) (10), which in turn have been shown to be a cause for aging in yeast (39). The stalled replication fork at the RFB seems to be a central intermediate in the processes of replication termination and recombination in the rDNA repeats. Therefore, we strove to investigate the molecular structure of the stalled replication fork. We found that the architecture of the stalled replication fork is strikingly different from the current model derived from progressing replication forks. The stalled replication fork exposes hardly any single-stranded DNA (ssDNA) and surprisingly, the nascent lagging strand is extended 3 bp farther than the nascent leading strand.

MATERIALS AND METHODS

Strains and culture conditions. *S. cerevisiae* A1 (*MAT***a** *ade2-101 ura3-52 his3*Δ*200 lys2-801* Δ*bar1::LYS2*) was used for all but one set of experiments, for which *S. cerevisiae* FTY23 (*MAT*α *ura3-52 his3-1 gal2gal10trp1 URA3*/YRpTRURAP) (43) was used to confirm the position of the arrested lagging strand at the RFB. Yeast cells, grown in complex medium (38) at 30°C to a density of about 6×10^6 cells/ml, were used as a source for rDNA isolation.

rDNA isolation and purification of replicative intermediates (RIs) by preparative 2D gel electrophoresis. Chromosomal DNA of the early-log-phase yeast cells was isolated (46) using conditions where RNA-DNA hybrids should remain intact, and the rDNA was enriched on CsCl gradients as described elsewhere (25). The enriched rDNA was digested with *Bgl*II (Axon Lab) and subjected to neutral/neutral two-dimensional (2D) agarose gel electrophoresis as described by Brewer and Fangman (5), with some modifications. Per slot, about 10 μg of the purified rDNA was loaded onto a 0.5% agarose gel (type II-EEO; Sigma) and run at 1 V/cm for 16 h in the first dimension. The second dimension was run in 1% low-gelling-temperature agarose (SeaPlaque; FMC) at 4 V/cm for 8 h. A gel slice was cut out at the position of the apex of the Y arc. Another gel slice was cut out at the position of the monomers. The DNA was recovered by digesting the agarose with AgarACE enzyme (Promega). In a 1.5-ml tube, a 250-mg gel slice was heated at 72°C for 5 min and cooled to 42°C, and then 0.5 U of agarase was added. The sample was further incubated at 42°C for 4 h, and the DNA was recovered by subsequent ethanol precipitation, with λ phage DNA added as carrier. Approximately 200 to 400 pg of intact replication forks were usually obtained per 2D gel.

* Corresponding author. Mailing address: Institut für Zellbiologie, ETH-Hönggerberg, CH-8093 Zürich, Switzerland. Phone: 41 1 633 33 42. Fax: 41 1 633 10 69. E-mail: sogo@cell.biol.ethz.ch.

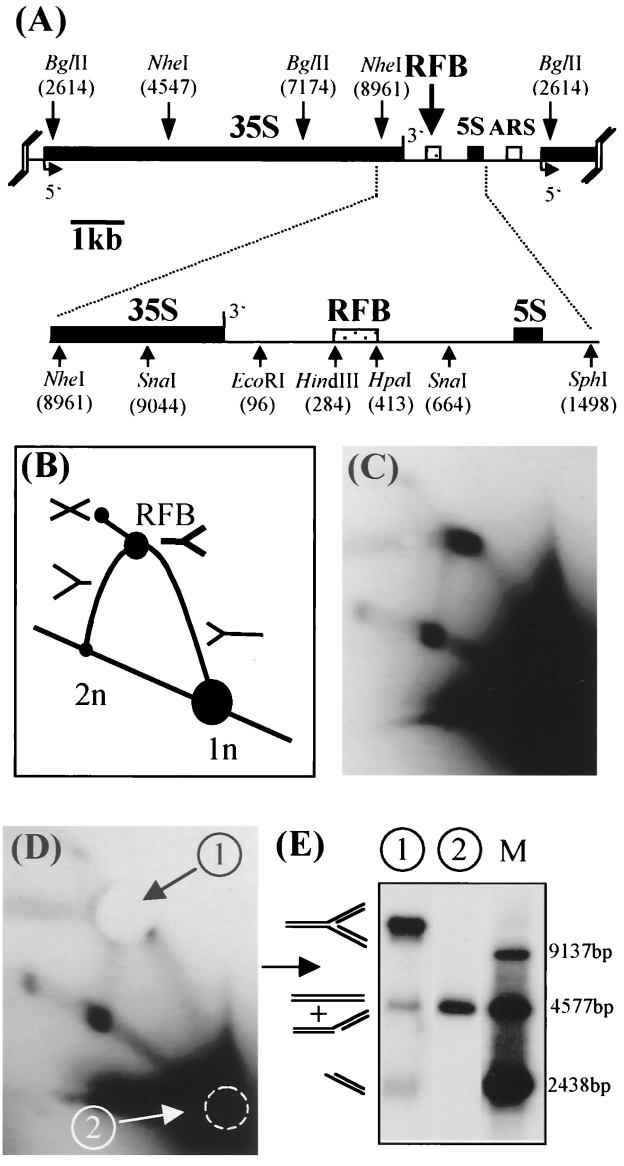

FIG. 1. Purification of replication forks stalled at the RFB by preparative 2D gel electrophoresis. (A) Structural organization and restriction map of an rDNA repeat unit (9.137 kb) of *S. cerevisiae*. Indicated are the 35S precursor, the 5S rRNA coding region (filled boxes), the ribosomal spacer region (thin line), the autonomously replicating sequence (ARS) element (open box), and the RFB (dotted box). The positions of relevant restriction sites are shown (numbers in brackets [40]). (B) Expected migration behavior of *Bgl*II-digested replicating rDNA (only the 4,577-bp fragment encompassing the RFB is depicted). (C) Southern blot analysis of *Bgl*II-digested rDNA separated on a 2D gel and hybridized to probe a (Fig. 2A). (D) Southern blot of a 2D gel used for purification of RIs stalled at the RFB (arrow 1) and linear monomers (arrow 2). Note that the gels shown in panels C and D were run in parallel. (E) Southern blot analysis of eluted RIs (lane 1) and linear monomers (lane 2). The rDNA fragments used as size markers (M) are shown.

Restriction enzyme, RNase H, and endo VII digests. Restriction digests were carried out in the conditions recommended by the supplier. All restriction enzymes were purchased from Axon Lab except for *Sna*I (isoschizomer *Bst*1077I), which was from MBI Fermentas. RNase H (MBI Fermentas) digestion of 1 μg of DNA (RIs plus carrier DNA) was performed for 30 min at 37°C in a total volume of 50 μl of restriction buffer (20 mM Tris-HCl [pH 7.8], 40 mM KCl, 8 mM $MgCl_2$, 1 mM dithiothreitol) including 4 U of enzyme. Endonuclease VII (endo VII) digestion of 1 μg of DNA (RIs plus carrier DNA) was performed for 30 min at 37°C in a total volume of 50 μl of endo VII buffer (50 mM Tris [pH 8], 10 mM $MgCl_2$, 50 mM NaCl, 1 mM dithiothreitol, 100 μg/ml of bovine serum albumin per ml) with various units of endo VII (a gift of B. Kemper).

Agarose gel electrophoresis and Southern transfer. Agarose gel electrophoresis was carried out in 1% agarose at 2 V/cm without ethidium bromide. The gels were alkaline transferred onto a Biodyne B membrane (Pall) and hybridized as described in reference 26. As hybridization probes, two PCR-amplified rDNA fragment (probe a, nucleotides [nt] 101 to 1088; probe b, nt 101 to 366 [see Fig. 2A]) and the 4,577-bp *Bgl*II rDNA fragment encompassing the RFB, previously subcloned into a pUC18 vector, were used. The probes were labeled with [α-^{32}P]dCTP (3,000 Ci/mmol; Amersham) using a random prime oligolabeling kit (Pharmacia) according to the manufacturer's instructions.

Primer extension. All primers were purchased from Mycrosynth. The sequences of the primers annealing to the top strand (parental leading and nascent lagging strands of the RIs stalled at the RFB) are as follows: primer 580, 5′-GGAACTTGCCATCATCATTC-3′ (nt 580 to 561); primer 483, 5′-CTCTT ACATCTTTCTTGGTA-3′ (nt 483 to 464). The sequence for primer 256, annealing to the bottom strand (parental lagging strand of RIs), is 5′-GATGGG TTGAAAGAGAAGG-3′ (nt 256 to 274). Primer end labeling and the primer extension reaction using *Taq* DNA polymerase (Perkin-Elmer Cetus) or Vent (exo−) DNA polymerase (New England Biolabs) were carried out as described previously (43), using 30 amplification cycles consisting of three steps: 94°C for 45 s, 55°C for 4 min, 72°C for 3 min. The DNA was precipitated by 0.1 volumes of 3 M sodium acetate and 4 volumes of ethanol. The primer extension products were fractionated on 6% polyacrylamide gel containing 50% urea and 1× Tris-borate-EDTA (35). Dideoxy sequencing (37) was carried out with CsCl-purified rDNA as the template using the same oligonucleotide as in the corresponding primer extension reactions.

Analysis of the nascent leading strand. 2D gel-purified RIs and monomers were digested to completion with *Bst*1077I (i-*Sna*I), the enzyme was removed with Strataclean (Stratagene), and the DNA was fractionated on a 6% sequencing gel containing 50% urea and 1× Tris-borate-EDTA. After polyacrylamide gel electrophoresis (PAGE), the DNA was transferred onto a nylon membrane by semidry electrophoresis (Bio-Rad) according to the instructions of the manufacturer. Finally, the membrane was sequentially hybridized with a strand-specific probe recognizing the nascent leading strand (and the parental lagging strand) of the RIs and one recognizing the nascent lagging strand (and the parental leading strand). The strand-specific probes were prepared by primer extension of a 248-bp PCR fragment (nt 418 to 666; amplified from rDNA with the primers denoted below) in the presence of [α-^{32}P]dCTP according to the protocol of Ruven et al. (34), using either primer 418 (5′-CAGGACATGCCT TTGATATGA-3′; nt 418 to 438) or primer 666 (5′-TACATGTATATATTGC ACTGG-3′; nt 666 to 646). Strand specificity of the probes was checked by hybridization to an rDNA restriction fragment (*Hpa*I/*Bst*AI) with one end blunt and the other 5 bp overhanging, which had been fractionated on a sequencing gel.

RESULTS

Isolation of RIs stalled at the RFB. We wished to explore the nature of the stalled forks at the RFB as precisely as possible. In a first step, we sought to map the positions of the nascent strands at nucleotide resolution. Hence, an important prerequisite for our study was the availability of highly purified RIs containing replication forks stalled at the RFB. The method we chose was preparative neutral/neutral 2D gels (25). In a first dimension, the DNA molecules are subjected to a neutral agarose gel electrophoresis under conditions that predominantly separate DNA molecules according to mass. Subsequently, the molecules are run at a 90° angle in another neutral agarose gel under conditions that separate DNA molecules mainly according to shape (5). As a result, linear molecules migrate along a diagonal, whereas RIs are retarded and migrate in specific, predictable patterns above the diagonal of the linear molecules. By digesting replicating rDNA with a restriction enzyme that cuts twice in the rDNA repeat, with one cutting site located close to the rDNA autonomous replication sequence element, mainly Y-shaped RIs will be generated. Such RIs migrate along an arc (the Y arc) as schematically depicted in Fig. 1B. If a particular RI accumulates because it occurs at replication pausing sites or replication fork barriers, a spot at its corresponding position on the otherwise smooth arc will appear.

rDNA enriched by cesium chloride density gradient centrifugation was digested with the restriction enzyme *Bgl*II, which cleaves twice in the rDNA repeating unit and gives rise to two

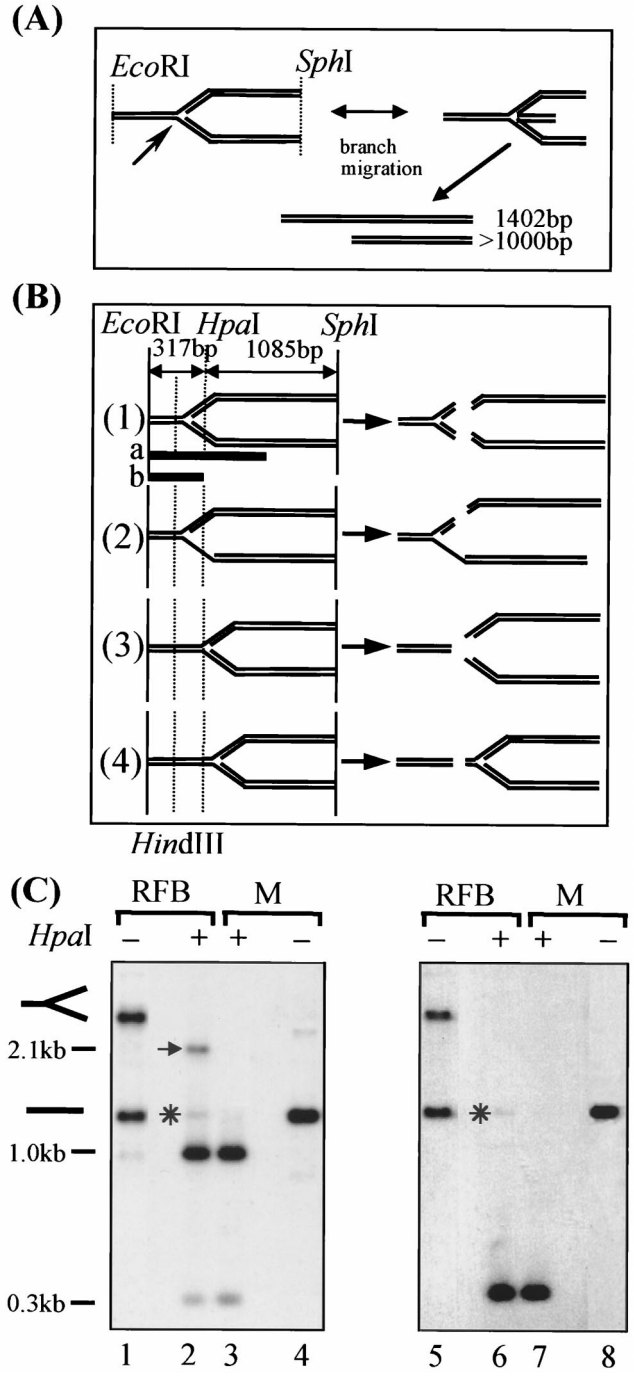

FIG. 2. *Hpa*I restriction analysis of replication forks stalled at the RFB. (A) Linear products that would result from branch migration at the stalled replication fork and the expected molecule sizes. Locations of the RFB (arrow) and the restriction cutting sites are indicated. (B) Schematic representation of possible products after redigestion of an RFB containing an *Eco*RI-*Sph*I fragment with *Hpa*I. Indicated are the probes (black bars) used to detect the *Hpa*I-*Sph*I (1,085 bp) and *Eco*RI-*Hpa*I (317 bp) fragments (a) or *Eco*RI-*Hpa*I fragment alone (b). The *Hin*dIII and *Hpa*I cleavage sites (dashed lines) are shown. Depending on the restriction products, the RFB could be localized either (i) between the *Hin*dIII and *Hpa*I sites, (ii) between the *Hin*dIII and *Hpa*I sites but with one of the daughter strands (most likely the lagging strand) containing a stretch of ssDNA, (iii) to the right of the *Hpa*I site, or (iv) farther to the right of the *Hpa*I site. (C) Southern blot analysis of the restriction products using a probe matching to the *Eco*RI-*Sph*I fragment (lanes 1 to 4) or to the *Eco*RI-*Hpa*I fragment (lanes 5 to 8). RI and monomers were either mock treated (lanes 1, 4, 5, and 8) or *Hpa*I digested (lanes 2, 3, 6, and 7). Bands interpreted as replication forks located to the right of the *Hpa*I restriction site (arrow) and RIs that possibly were not cut in the lagging strand (asterisks) are indicated. The size markers (M) were derived from hybridization of probe a to rDNA restriction fragments (*Eco*RI/*Hpa*I, 0.3 and 2.1 kb; *Eco*RI/*Alw*NI, 1.0 kb). Note that in lane 1, even after overexposure of the autoradiograph, only traces of fragments of about 1 kb were detectable (for details see text).

fragments of equal length (Fig. 1A). The RFB, located in the center of one of these fragments, leads to an accumulated Y-shaped RI with three arms of almost equal lengths migrating at the apex of the Y arc (intense spot in Fig. 1C). In order to isolate replication forks stalled at the RFB, a gel slice at the position of the intense spot at the apex of the Y arc was cut out of the 2D gel (Fig. 1D). A second gel segment was cut out at the position where nonreplicating linear *Bgl*II fragments run (in this study referred to as the monomers; 1n in Fig. 1B). Subsequently the DNA was recovered from the agarose slice. Closer inspection of an aliquot of the 2D gel-purified RIs revealed that the purified DNA invariably consisted of three populations with different electrophoretic mobilities (Fig. 1E). The major product with the slowest mobility represents intact replication forks stalled at the RFB, as judged by its electrophoretic mobility and because it is sensitive to T4 endo VII (see below). One of the two other products shows the same migration as does linear monomer DNA, and the third product migrates at a position expected for one of the three arms of the RI. We therefore assume that the two lower bands represent breakdown products of replication forks, most likely resulting from shear breakage at the fork junction rather than branch migration (Fig. 2A; see below).

It has been shown that exclusively leftward-moving forks are arrested at the RFB (5, 22, 25). Therefore, we expected the isolated RIs to consist mainly of stalled replication forks that had traveled leftward. However, replication is initiated in only one of out of five or more rDNA repeating units (5, 22, 42). The other units are replicated by rightward-moving replication forks. Consequently, the position of the RFB spot on the 2D gel is overlapped by a part of the Y arc that consists of rightward-moving replication forks. Such forks are inevitably copurified with the leftward-moving forks because of their similarities in mass and shape. To assess the fraction of rightward-moving replication forks present in the 2D-gel-purified DNA, we redigested the purified DNA with *Nhe*I, which cuts 460 bp upstream of the *Hin*dIII-*Hpa*I fragment. As a result, rightward-moving replication forks that are cut in the newly synthesized arms migrate close to the linear restriction fragment, whereas leftward-moving forks, having an almost doubled mass, migrate substantially more slowly. Southern blot analysis of *Nhe*I-digested, gel-isolated RIs revealed that less than 5% of the purified RIs consisted of rightward-moving replication forks (data not shown). These forks should not interfere with subsequent analyses.

Analysis of the isolated RIs with the restriction enzyme *Hpa*I. As a first step toward high-resolution mapping of the RFB, we analyzed the purified RIs with a restriction enzyme cutting close to the arrest site of the stalled replication fork. The branch point of the replication fork, stalled at the RFB, has been mapped to a position in the vicinity of the *Hpa*I restriction site (6, 19, 25). Theoretically, digestion of RIs with *Hpa*I could give four different results depending on where the branch point of the fork was located with respect to the *Hpa*I restriction site (schematically depicted in Fig. 2B). A combination of these results is also conceivable, because the replication forks stalled at the RFB may not be homogenous in the position of the branch point. First, the replication fork could be blocked between the *Hin*dIII and *Hpa*I sites, resulting in both

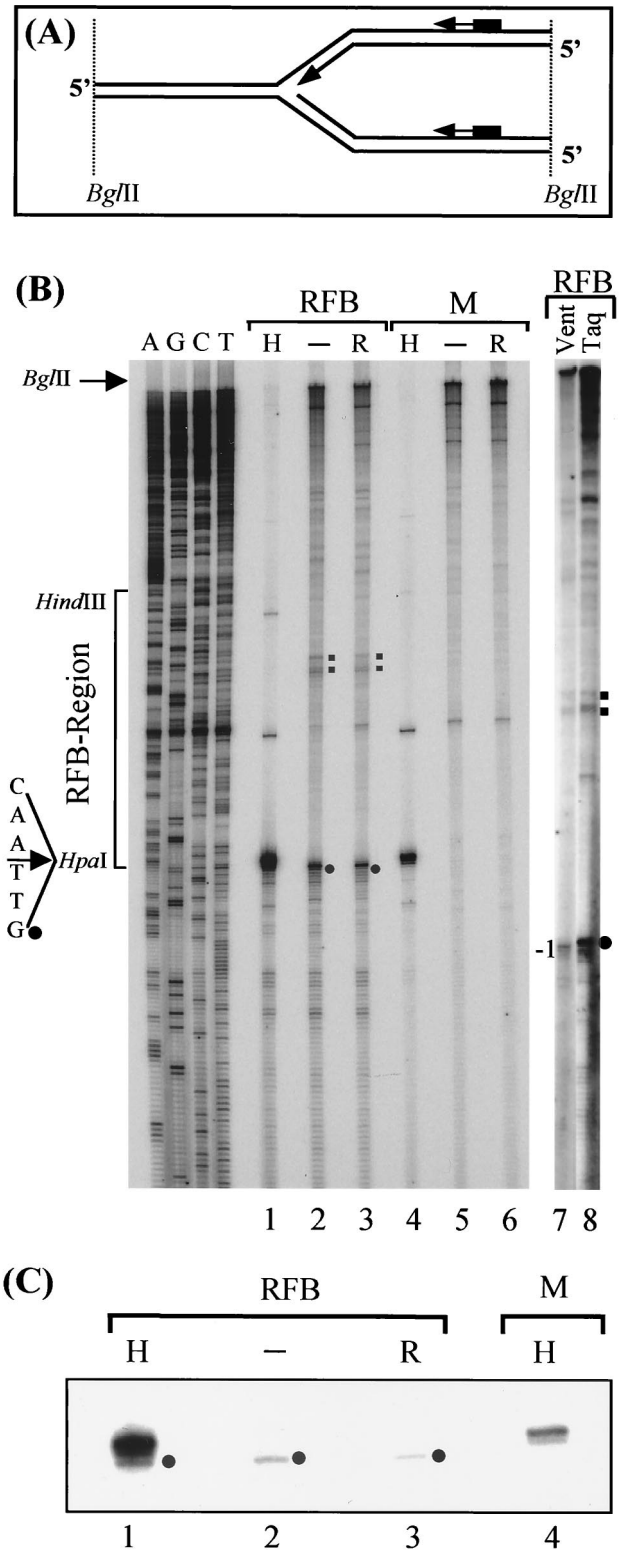

FIG. 3. Mapping of the lagging strand arrest site at the RFB by primer extension. (A) Illustration of the strategy for mapping the lagging strand arrest site by primer extension using primer 580 (see text for details). (B) PAGE separation of primer extension products. Either RIs (RFB; lanes 1 to 3, 7, and 8) or monomers (M; lanes 4 to 6) were used as templates. Prior to the primer extension, the *Bgl*II-digested template DNA was either treated with *Hpa*I (H; lanes 1 and 4), mock treated (lanes 2 and 5), or treated with RNase H (R; lanes 3 and 6). Primer extension was done using *Taq* (lanes 1 to 6 and 8) and Vent (exo-) lane 7) polymerases. Indicated are the major block site (filled circle), the minor block sites (filled squares) for the polymerase extension reaction, and the DNA sequence of the template strand (lanes A, G, C, and T). (C) Enlargement and shorter exposure of a part of the sequencing gel as shown in panel B. Note that the distances from primer 580 to the *Bgl*II and *Hpa*I sites are 2,543 and 167 bp, respectively (not indicated).

leading and lagging strands being but by *Hpa*I (Fig. 2B, sketch 1). Second, the *Hpa*I site could be located in a stretch of ssDNA on the lagging strand. In this case, *Hpa*I would cut only the leading strand (Fig. 2B, sketch 2). Third, the approaching replication fork could be blocked just a few base pairs before reaching the *Hpa*I restriction site. The cleaved RIs would break down into linear DNA molecules if the double-stranded region sealing the two arms was short enough (Fig. 2B, sketch 3). Fourth, the replication fork could be stalled before it reaches the *Hpa*I restriction site (Fig. 2B, sketch 4).

2D gel-purified RIs containing arrested replication forks and, as a control, similarly purified monomers, were first digested with *Eco*RI and *Sph*I. Subsequently, aliquots of the RIs as well as the monomers were digested with *Hpa*I and analyzed by Southern blotting (Fig. 2C). Inspection of the *Eco*RI-*Sph*I-cut RIs clearly revealed that the isolated material contained not only RIs (slow-migrating band in lane 1) but also a monomer contamination (prominent faster-migrating band in lanes 1 and 4) that accounts for about 60% of the material (compare the relative intensities of both bands in lane 5). This monomer contamination is probably due to overloading of the 2D gel with monomers. If the monomers arose from branch migration that occurred during the digestion or isolation of the RIs, the extruded nascent strands would give rise to an additional band of about 1.0 kb (Fig. 2A). However, in lane 1 only a very faint band close to the detection level is found at this position, and it might even represent breakdown products of RIs.

Digestion of the RIs stalled at the RFB with *Hpa*I gives rise to four bands. Two of them appear in the digest of the monomers (compare lanes 2 and 3 in Fig. 2C). The two more rapidly migrating products can be explained assuming that the RIs are digested as depicted in sketch 3 of Fig. 2B. Therefore, the location of the branch point of the replication fork must be in the vicinity of the *Hpa*I restriction site.

About 15% of the digested RIs gave rise to a retarded band which cannot be detected by a probe hybridizing to the left of the *Hpa*I site (Fig. 2C, compare lanes 2 and 6). This band can be explained only with replication forks stalled to the right of the *Hpa*I site (Fig. 2B, sketch 4). A very faint signal (less than 5% of the total signal for the RIs stalled at the RFB) appeared at the mobility of the linear molecules. This signal was also detected by the probe hybridizing to the left of the *Hpa*I site and could be explained by the presence of a single-stranded stretch over the *Hpa*I site on the lagging strand of the replication fork (Fig. 2B, sketch 2). Taken together, the *Hpa*I digest data indicate that the majority of the 2D-gel-purified RIs consists of a replication fork blocked close to the *Hpa*I restriction site and that on the lagging strand there are only very few stretches of ssDNA that overlap the *Hpa*I restriction site. A minority of the RIs, however, consist of forks that are located to the right of the *Hpa*I restriction site.

The nascent lagging strand is blocked at position 418 (first base of the *Hpa*I restriction site) and at two additional minor sites located toward the *Hin*dIII site. To obtain a higher resolution, we carried out a primer extension-based assay. The experimental strategy of this assay is shown in Fig. 3A. A 5′-end-labeled primer is annealed to the replicated branches of the RIs. Subsequently, in a linear amplification reaction using

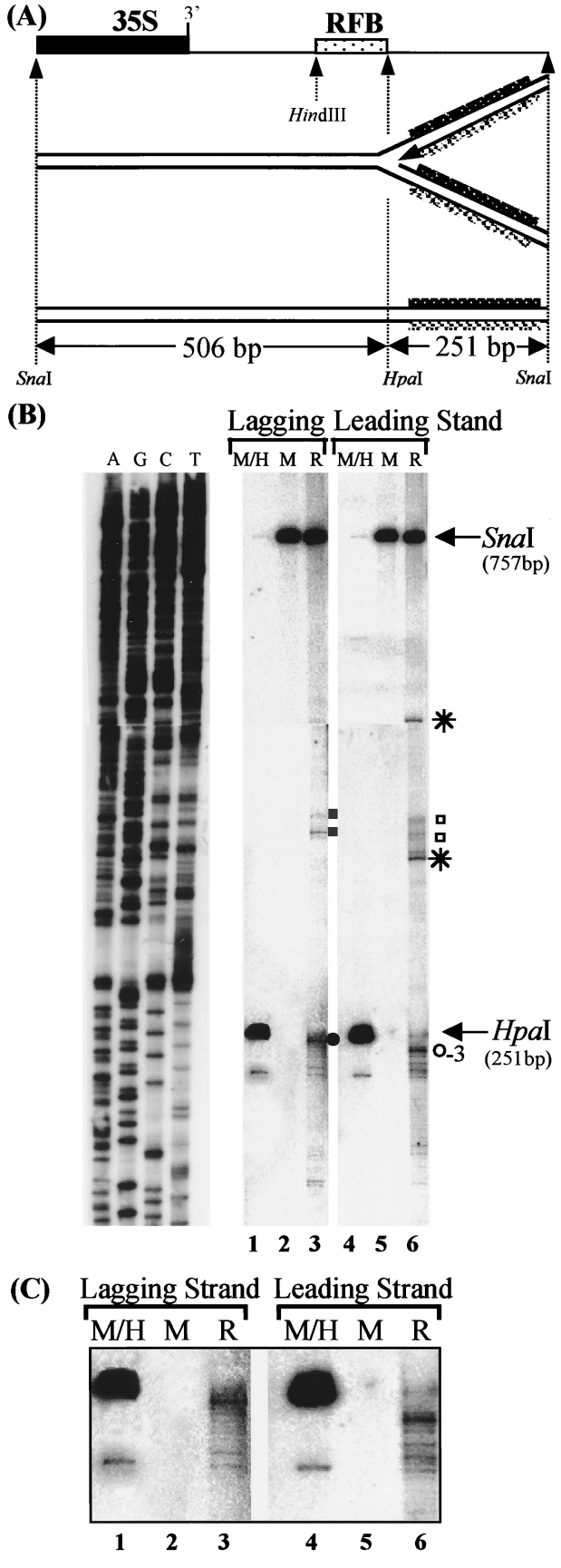

Taq polymerase, the primer is extended to the 5′ end of the nascent lagging and the 5′ end of the parental leading strand. The denatured primer extension products are finally fractionated on a sequencing gel. Note that the result consists always of a composite pattern of the two template strands read by the *Taq* polymerase. Therefore, a primer extension of the isolated nonreplicating monomers is always run in parallel as a control. Consequently, primer extension products that are observed only in reactions with RIs as templates can be assigned to the nascent lagging strand. Since RIs of replication forks stalled at the RFB are long-lived molecules in comparison to RIs of moving forks, we expected the majority of the Okazaki fragments on the lagging strand to be processed and ligated. Therefore, the mapped position of the 5′ end of the lagging strand should coincide with the point of arrest of the lagging strand at the RFB.

*Bgl*II-digested, 2D-gel-isolated RIs and monomers were used as templates for the extension of primer 580 (see Materials and Methods). The extension products were subsequently fractionated on a sequencing gel (Fig. 3B, lanes 2 and 5). As an internal control, aliquots of the RIs and monomers were digested with *Hpa*I prior to the primer extension (Fig. 3B, lanes 1 and 4). Primer extension of RIs gives rise to a set of bands that do not appear in the primer extension of the monomer (Fig. 3B, compare lanes 2 and 5). The most prominent of these bands denotes the major lagging strand block site of the stalled fork at the RFB. As expected from the results of the *Hpa*I digest presented in Fig. 2, the block site maps very closely to the *Hpa*I restriction site, namely, to the G at position 418, the first base of the *Hpa*I recognition sequence (compare lanes 1 and 2 in Fig. 3B or, for a lower exposure, in Fig. 3C). Interestingly, the restriction enzyme *Hpa*I is still able to cut the RIs, despite the close vicinity of the replication fork. There are a number of shorter primer extension products below the signal of the major stop. These signals, which account for about 20 to 30% of the total signal from the nascent lagging strand as quantified by a PhosphoImager, could be due to approaching replication forks that have not yet reached the main stop. This notion is supported by the *Hpa*I digest of RIs (Fig. 2), where about 10 to 20% of the RIs seem to consist of forks that have not yet reached the *Hpa*I site. An alternative explanation for these minor bands would be that they result from Okazaki fragments not yet fully processed.

There are two additional signals toward the *Hin*dIII site present in primer extension reaction of RIs at positions 330 to 340 (Fig. 3B, lane 2). These signals probably derive from two minor stop sites that have already been observed by Brewer et al. (6). Primer extension with primer 483 annealing 97 bp farther downstream than primer 561 (see Materials and Meth-

FIG. 4. Mapping of the leading strand arrest site by Southern blot analysis. (A) Restriction map showing the 757-bp *Sna*I fragment encompassing the RFB. A replication fork stalled at the RFB and the corresponding monomer are shown below. Strand-specific probes used to detect the leading (black bar) and lagging (grey bar) strands are indicated. (B) Southern blot analysis of RIs separated by PAGE. After electrophoresis, the gel was cut into similar-size upper and lower parts and electroblotted onto a nylon membrane. The membrane was sequentially hybridized with a strand-specific probe detecting the nascent lagging strand (lanes 1 to 3) and with a strand-specific probe detecting the nascent leading strand (lanes 4 to 6). Indicated are monomers (M), *Hpa*I-digested monomers (M/H), the RFB (R), bands corresponding to the *Hpa*I/*Sna*I and *Sna*I/*Sna*I restriction fragments (arrows), the major (circles) and minor (squares) block sites for the leading and lagging strands, and bands detected only with the probe specific for the nascent leading strand (asterisks). To the left, the DNA sequence of a size marker (lanes A, G, C, and T; generated by primer extension of primer 256) is shown. Note that the fragments of the restriction digests and the shown DNA sequences cannot be directly aligned. (C) Enlargement of the major block site of the lagging and leading strands.

ods) confirmed this mapping (data not shown). The same results were also obtained using yeast strain FTY23 (43) instead of A1 (data not shown). We therefore conclude that the position of the block that we mapped is not strain dependent.

The stalled nascent lagging strand at the RFB is devoid of the RNA primer. Next, we wished to find out whether we mapped the 5′ position of the last RNA primer on the lagging strand, or whether the RNA primer had already been processed at the stalled replication fork. *Taq* polymerase is known to possess a weak reverse transcriptase activity (31). For this purpose, prior to the primer extension reaction we digested an aliquot of the RIs with RNase H, which specifically digests RNA in DNA-RNA hybrid. The resulting primer extension products were identical to those obtained when untreated RIs were used as templates (Fig. 3B, compare lanes 2 and 3). This result indicates that we mapped the 5′ DNA end of the nascent lagging strand. However, since we do not have a positive control for the RNase H, we performed an additional primer extension using another thermostable DNA polymerase, the Vent (exo-) polymerase, and compared the products with the ones of the *Taq* polymerase. The Vent (exo-) polymerase is known to be unable to use RNA as a template and therefore reads only to the DNA-RNA junction of an RI (3). Both DNA polymerases gave rise to virtually identical primer extension products, except that the product of the major stop site seems to be one base shorter when elongated with Vent (exo-) polymerase (Fig. 3D). However, this difference results most likely from the terminal transferase activity of the *Taq* polymerase, which is much weaker in the case of the Vent (exo-) polymerase (31). If the *Taq* polymerase were extended until the 5′ end of the last RNA primer, the product would be approximately 10 bp longer than the one of the Vent (exo-) polymerase, because the average length of an RNA primer used for initiation of Okazaki fragment synthesis in eukaryotes has shown to be about 10 bp (7). Clearly, we have not mapped the 5′ end of such an RNA primer. If we assume that the RNA primers were partially degraded during DNA isolation, a reverse transcriptase activity of the *Taq* polymerase should lead to two populations of extension products arising from templates with and without an RNA primer. Although only one population of products was found, we cannot rule out the possibility that the RNA primer is present but not detectable in our assay. The *Taq* polymerase could have stopped at the DNA-RNA junction on the nascent lagging strand. However, in this case the RNA primer would extend over the *Hpa*I restriction site, making cleavage of the lagging strand by *Hpa*I impossible. The results of the *Hpa*I digestion shown in Fig. 2 clearly contradict such assumptions. Therefore, we conclude that the Okazaki fragments on the lagging strand of the replication fork stalled at the RFB are fully processed and the last RNA primer is removed after the replication fork has reached the RFB.

The nascent leading strand and the nascent lagging strand are stalled at positions very close to each other. Since the elongation point of the nascent leading strand cannot be mapped by primer extension, we had to devise another method to map the arrest site of the leading strand. Therefore, we decided to use an assay loosely related to an indirect end-labeling assay. First, the purified RIs blocked at the RFB were digested with *Sna*I, which generates a 757-bp DNA fragment encompassing the RFB. The fragments were then fractionated on a denaturing 6% acrylamide–7 M urea gel and subsequently electrotransferred onto a nylon membrane. Finally, the membrane was hybridized with a strand-specific probe close to the *Sna*I restriction site (Fig. 4A). A probe specific for the top strand will detect the parental leading as well as the nascent lagging strand, a probe specific for the bottom strand, the parental lagging strand, and the nascent leading strand. The signals for the parental strands will be detected at the position of 757 bp; the nascent strands will be shorter. Therefore, the precise location(s) of the nascent strands can be deduced from their size. To identify potentially interfering bands from nicked DNA, nonreplicating, *Sna*I-cut DNA was run in parallel as a control.

Figure 4B shows a Southern blot with nucleotide resolution of *Sna*I-digested replication forks stalled at the RFB that were fractionated on a sequencing gel. The membrane was first hybridized with a probe specific for the top strand (lanes 1 to 3). The membrane was subsequently stripped and rehybridized with a probe specific for the bottom strand (lanes 4 to 6). As a background control, nonreplicating monomers were treated exactly like the RIs and run in parallel (Fig. 4B, lanes 2 and 5). Additionally, *Hpa*I-digested monomers were run on the same gel as an internal size marker (Fig. 4B, lanes 1 and 4). As expected, using the strand-specific probe for the nascent lagging strand, we detected the major arrest site of the stalled replication fork at position 418 and the two minor arrest sites toward the *Hin*dIII site (Fig. 4B). These results are in good agreement with the mapping of the blocked replication fork at the RFB by primer extension.

The probe specific for nascent leading strand shows a major arrest site in the vicinity of the *Hpa*I restriction site, very close to the position of the lagging strand block site. Unexpectedly, the major arrest site of the leading strand is located three bases downstream of the lagging strand, at position 421; there are also at least two minor arrest sites, mapping to positions close to those of the minor lagging strand blocks. However, two more bands appear at positions at which no corresponding bands for the lagging strand are present (Fig. 4B). The upper band corresponds to a position outside of the *Hpa*I-*Hin*dIII fragment and is therefore unlikely to be the product of a stalled replication fork at the RFB. However, the faster-migrating band could be interpreted as the product resulting from an additional arrest site of the leading strand. The corresponding nascent lagging strand could be blocked at position 418 bp, thereby exposing a 85-bp stretch of ssDNA, or it could be blocked at one of the minor arrest sites. In the first case, a fraction of the replication forks stalled at the RFB would expose a stretch of ssDNA, which contradicts the results of the *Hpa*I analysis of the RIs presented in Fig. 2.

We conclude from these data that the majority of the leading and lagging strands of the stalled replication fork at the RFB are extended to very similar positions, with the nascent lagging strand being three bases ahead of the nascent leading strand (Fig. 5).

T4 endonuclease VII discriminates between the leading and lagging strands. There are a number of DNA-modifying enzymes specific for branched DNA molecules (for reviews, see references 16 and 44). Such enzymes could be useful tools to characterize and analyze RIs in combination with the primer extension assay described in this study. T4 endo VII, one of these enzymes, is exceptional in its ability to use a large number of branched DNA structures and/or structural perturbations in DNA as substrates (reviewed in reference 16). These include, among others, three-way junctions (Y structures) such as occur at the replication fork during DNA replication. Endo VII has been shown to resolve a variety of synthetically constructed Y structures into linear molecules by introducing nicks 3′ to the junction (15, 33). To our knowledge, however, endo VII cleavage of naturally occurring RIs has not been investigated so far. A major difference between the naturally occurring RIs and the synthetic Y structures are the two homologous

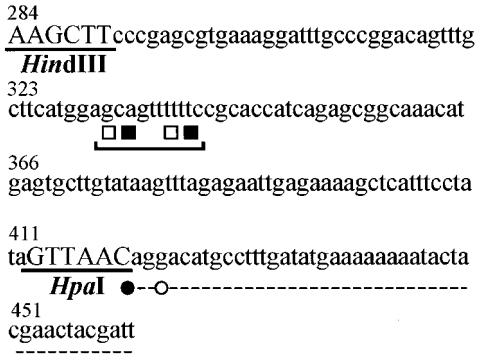

FIG. 5. Nucleotide sequence of the template strand containing the *Hin*dIII-*Hpa*I fragment and downstream flanking region. Indicated are the mapped positions of the major (circles) and minor (squares) blocks found in nascent lagging strand (filled symbols) and the nascent leading strand (open symbols) of the stalled replication fork. The minor blocks may not be exactly at the indicated nucleotide but rather over the region indicated by the bracket.

arms of RIs, because the synthetic Y structures investigated so far consisted of three nonhomologous arms.

To resolve RIs into linear DNA molecules, at least one nick has to be introduced in the vicinity of the branch point, in either the parental leading or the parental lagging strand. These nicks can be detected by primer extension. A primer annealing to the unreplicated part of a given RI detects the introduced nicks in the parental lagging strand; one annealing to the replicated arms detects the nicks in the parental leading strand (Fig. 3A; see also Fig. 6B and C). Note that the primer extension products of the parental leading strand will be accompanied by the products of the nascent lagging strand.

*Bgl*II-digested, 2D-gel-purified rDNA consisting of about 50% RIs and 50% linear monomers (not shown) was redigested with *Eco*RI and *Sph*I (Fig. 6A, lane 1) in order to produce asymmetrical RIs with a short unreplicated arm and two long replicated arms (Fig. 6A, diagram). Subsequently, the RIs and monomers were treated with increasing amounts of endo VII (Fig. 6A). A 200-U aliquot of endo VII was sufficient to resolve the Y-shaped RIs completely (Fig. 6A, lane 4). The retarded band of the RIs has disappeared completely, giving rise to two faster-migrating products: one comigrating with the linear monomers and a shorter product, migrating at the size of a replicated arm of the RI. This suggests that one of the replicated arms was released. In short, this experiment indicates that only one of the replicated arms at a time, either the leading or the lagging arm, is cleaved by endo VII (Fig. 6A, diagram). However, this experiment does not give us any clue about which strand is released by endo VII. Does endo VII cut randomly in the leading and the lagging strand, resulting in release of 50% leading and 50% lagging strand? Is there a preference for one of the strands, or does endo VII release only one strand, thereby cleaving either leading or lagging strand? To answer these questions, we employed the primer extension assay using aliquots of the RIs digested with 200 U of endo VII as templates. First, primer 256 (see Materials and Methods), which anneals to parental lagging strand in the unreplicated part of the RIs, was elongated to detect cleavage in the lagging strand. The primer extension products were fractionated on a denaturing polyacrylamide gel, and the products of reactions with endo VII treated RIs were compared to the products of reactions with untreated RIs. No bands indicative of endo VII cleavage in the parental lagging strand were observed (Fig. 6B, compare lanes 1 and 2). This result strongly implies that endo VII degrades the RIs by cutting exclusively in the parental leading strand.

In a next step, we carried out a primer extension using primer 580 (see Materials and Methods), which anneals to the parental leading and nascent lagging strand and therefore detects cuts in both the parental leading and nascent lagging strands. Figure 6C shows the primer extension products fractionated on a denaturing polyacrylamide gel. In contrast to the previous primer extension, endo VII treatment gives here rise to a stretch of bands with similar intensities over 11 nt close to the *Hpa*I site (lane 2). In untreated RIs (lane 1), six prominent bands are observed close to the *Hpa*I site. The most slowly migrating product, corresponding to the major stop of the lagging strand at the RFB, gives rise to the strongest signal (better visible on the enlargement of a shorter exposure of the gel). The mobility of this product indicates that it is one nucleotide longer than the corresponding largest product among the series from the endo VII treated RIs, indicating that the nascent lagging strand was attacked by endo VII. This seems plausible, because the incisions in the nascent lagging strand seem to occur over maximally 11 nt and are 3′ to the junction. Endo VII has been shown to cut over 2 to 6 nt 3′ to the junction (33). However, the observed signals close to the *Hpa*I site in endo VII-treated RIs must also be due to cleavage in the parental leading strand, because this strand is released by endo VII treatment. Since the nascent leading strand maps to a position of three nucleotides behind of the branch point, as shown in this study, incisions 3′ to branch point on the parental leading strand give rise to products very similar to the ones from the nascent lagging strand. This is what we actually observe. Taken together, our data strongly suggest that endo VII cuts exclusively in the homologous, replicated arms of RIs (as depicted in Fig. 6D, diagram). As a consequence, the leading arm of an RI can be selectively removed with the help of endo VII.

DISCUSSION

By means of preparative 2D gel electrophoresis, we were able to isolate a population of DNA molecules consisting almost exclusively of replication forks stalled at the RFB, and we have analyzed their structure at nucleotide resolution. Primer extension analysis of the nascent lagging strand revealed a major arrest site at position 418 and at least two minor arrest sites toward the 3′ end of the rDNA transcription unit, at positions 330 to 340. The Okazaki fragments on the lagging arm are fully processed, with no RNA primer being attached to the last Okazaki fragment. An indirect end-labeling assay revealed that the major arrest site of the leading strand is located at position 421, three bases behind the nascent lagging strand. Thus, the replication fork stalled at the RFB hardly exposes any ssDNA on its newly synthesized arms. Finally, by digestion of the isolated replication forks with endo VII, we were able to specifically release the leading arm from the RIs. Thus, endo VII could be a useful tool for the characterization of RIs.

Locations of the arrest sites of the stalled RIs at the RFB. The location of the RFB has previously been mapped at low resolution by two independent assays: by 2D gel electrophoresis (6, 19) to a 129-bp fragment between the *Hin*dIII and *Hpa*I restriction sites (positions 286 to 415 [Fig. 1]) and by electron microscopy (EM) (25) to position 376 ± 70 bp. Furthermore, the minimal sequences required for the block of the replication fork seem to reside within this fragment (6, 19). We mapped the major arrest point to a position three bases in front of the *Hpa*I cutting site, overlapping the first nucleotide of its recognition sequence. Even though the block that we mapped is not

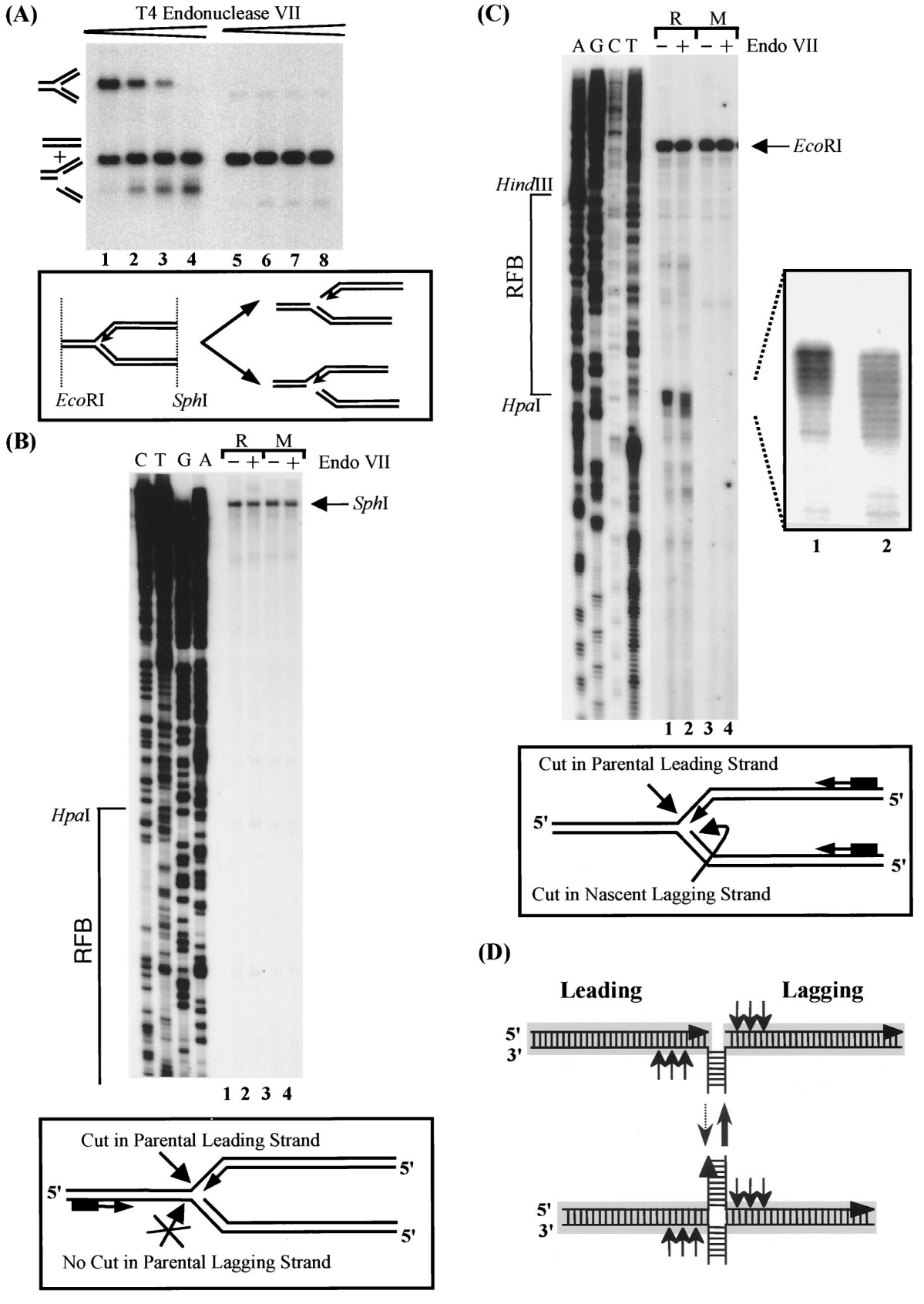
(A)
T4 Endonuclease VII
1 2 3 4 5 6 7 8
EcoRI
SphI
(B)
C T G A
R M
– + – +
Endo VII
SphI
HpaI
RFB
1 2 3 4
Cut in Parental Leading Strand
5'
No Cut in Parental Lagging Strand
(C)
A G C T
R M
– + – +
Endo VII
EcoRI
HindIII
RFB
HpaI
1 2
1 2 3 4
Cut in Parental Leading Strand
5'
Cut in Nascent Lagging Strand
(D)
Leading
Lagging
5'
3'

located within the *Hpa*I-*Hin*dIII fragment, our result is consistent with the previous mappings. Since the restriction enzyme *Hpa*I is still able to cut the DNA, the two arms of the stalled replication will be released and the spot of the accumulated RIs will disappear on the 2D gel upon *Hpa*I digestion.

Because of its close vicinity to the stalled replication fork at the RFB, the *Hpa*I digestion provides us with valuable information about the structure of the isolated replication forks. Digestion of the isolated RIs with *Hpa*I resulted in a slower-migrating product, comprising 10 to 20% of the isolated RIs. These products can be explained by the presence of replication forks located in front of the *Hpa*I restriction site. This notion was confirmed in the primer extension analysis by the appearance of a series of bands below the major signal of the 5′ end of the nascent lagging strand. These bands are most likely due to the approaching replication forks that are just about to reach the RFB. Alternatively, they could be due to various minor arrest sites in front of the major arrest at position 418. However, we favor the first interpretation, because the presence of such approaching forks in the gel-isolated material is to be expected considering the low resolution of the 2D gel electrophoresis. The relatively high contribution of 10 to 20% to the long-lived stalled replication forks at the RFB could be indicative of a slowing down of the replication forks in front of the RFB, and the pattern of the primer extension product could reflect individual Okazaki fragments.

Upon close inspection of the spot arising from the accumulated replication forks stalled at the RFB, Brewer et al. observed a somewhat elongated signal that appeared to consist of two discrete spots of different intensities (6). The origin proximal spot was more intense and most likely coincides with the major block that we have detected at position 418. Likewise, we have observed at least two closely spaced minor block sites, about 90 bp closer to the *Hin*dIII site than the major arrest site. The position and intensity of these minor spots strongly suggest that these two stops correspond to the other weaker spot observed by Brewer et al. (6). Whereas at least two stops are detected by primer extension, only one will be detected by 2D gel electrophoresis, because the two arrest sites are too closely spaced to be resolved. It still remains to be elucidated whether the major and minor stop sites are alternative arrest sites or whether a given replication fork is sequentially stalled at the major and one or both minor stop sites (6). In the first case, fewer replication forks would be stalled at the minor block sites, whereas in the second case the replication fork would be blocked for a shorter period at the minor sites.

The processing of the lagging strand. Primer extension of the RIs stalled at the RFB gave rise not to a population of primer extension products distributed over a broad region but rather to a single predominant product. This finding indicates that the majority of the replication forks stalled at the RFB are fully processed. Since the stalled replication forks at the RFB are long-lived RIs that remain halted at the RFB up to several minutes (assuming that the speed of the fork movement is constant and approximately 50 bp/s), there is sufficient time to complete the processing of the last Okazaki fragment. In the simian virus 40 system, the maturation of the Okazaki fragment is known to take about 1 min (11). Furthermore, since the fusion of two adjacent replicons in the rDNA takes place at the RFB, it seems that the stalled nascent lagging strand does not need further modification before the ligation with the nascent leading strand from the opposite moving fork.

Similar position of the nascent strands at the RFB. A remarkable feature of the stalled replication fork at the RFB in *S. cerevisiae* is its lack of ssDNA on the newly synthesized lagging arm. Besides the data presented in Fig. 4, there are three additional lines of evidence suggesting that the stalled replication fork at the RFB does not expose a significant stretch of ssDNA on the lagging strand. First, when RIs were enriched by benzoylated naphthoylated DEAE-cellulose, a considerable amount of the accumulated RIs from the RFB eluted together with the nonreplicating, linear DNA molecules in the salt wash (22). This indicates that the blocked replication forks at the RFB expose less ssDNA than progressing replication forks. Second, in a study of the chromatin structure of replication forks stalled at the RFB by EM, the DNA immediately behind the forks appeared mostly double stranded (25). Finally, the *Hpa*I digest presented in this study suggests that the leading strand is not extended beyond the *Hpa*I restriction site, because in this case *Hpa*I could not cleave in the single-stranded lagging arm. Together, the position of the RFB (see Results) and the structure of the arrested forks (absence of large single-stranded regions) match with the data obtained from the analysis of *in vivo* psoralen-cross-linked RIs by EM (25). Since psoralen-cross-linked DNA should not undergo transitions in the DNA structure (e.g., branch migration or strand displacement), we must assume that the basic architecture of the RIs remained unaltered during the isolation procedure described here.

Another salient feature of the stalled replication fork at the RFB is the position of the 5′ DNA end of the processed nascent lagging strand, which is located three bases ahead of the 3′ end of the nascent leading strand. This finding raises intriguing questions about the molecular mechanism of the replication fork block at the RFB. We propose a model (Fig. 7) exploiting the asymmetry of the replication fork to explain this finding. Contrary to the continuously synthesized nascent leading strand, the nascent lagging strand is known to be synthesized discontinuously in the direction opposite the replication fork movement by Okazaki fragments, in eukaryotes of 40 to 300 bp in size (11). These fragments can be synthesized only by elongation of an initiator DNA (iDNA), consisting of a RNA-DNA primer generated by the DNA polymerase α (polα)/primase (29; for a review, see reference 41). The iDNA has an average length of about 40 bp, of which about 10 bp consists of RNA. Thus, relative to the 5′ end of last primer of the lagging strand, the nascent leading strand was blocked at least 10 bp earlier.

Recent advantages in the enzymology of the eukaryotic replication fork have revealed its basic architecture (for reviews,

FIG. 6. Endo VII digestion and subsequent primer extension analysis of stalled RI. (A) Southern blot analysis of *Eco*RI- and *Sph*I-digested RIs plus monomers (50%/50% ratio; lanes 1 to 4) and monomers alone (lanes 5 to 8) treated with increasing amount of endo VII (0, 10, 50, and 200 U). Probe a (Fig. 2A) was used for detection. An interpretation of the digestion products is drawn below. The appearance of two digestion products indicates that the leading and/or lagging strand of the RI was released by endo VII. (B) Primer extension analysis of the parental lagging strand using primer 256. Top, PAGE separation of primer extension products. RIs (R) or monomers (M) were either treated with endo VII (lanes 2 and 4) or mock treated (lanes 1 and 3). The *Hpa*I-*Hin*dIII fragment is depicted to the left. Bottom, schematic representation of an RI showing the annealing position of the primer as well as the presumed cutting sites of the endo VII. Note that the distance from primer 256 to the *Sph*I site is 1,242 bp (not indicated). (C) Primer extension analysis of the parental leading strand using primer 580. Details are as for panel B. Note that the distance from primer 580 to the *Eco*RI site is 676 bp (not indicated). Right, enlargement of a part of the sequencing gel; bottom, annealing positions of the primer and the presumed cutting sites of endo VII. (D) Schematic representation of the postulated Holliday-like DNA structure for the stalled replication forks at the RFB. Arrows indicate the potential endo VII cleavage sites. Homologous arms are depicted in grey.

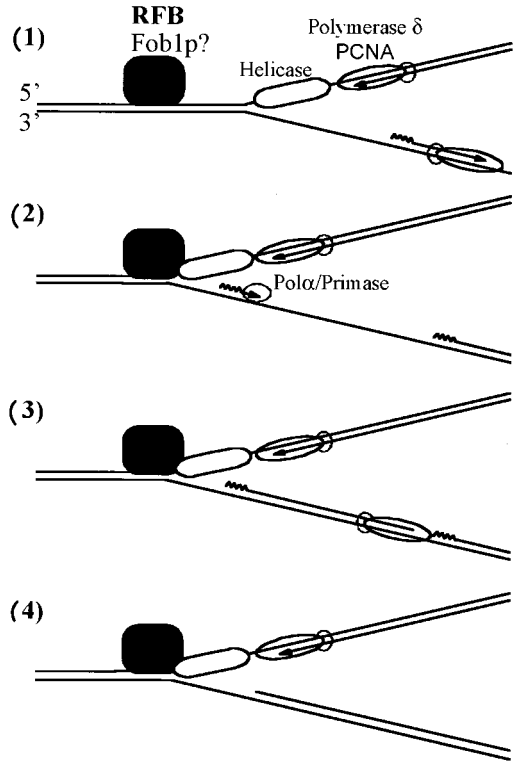

FIG. 7. Model illustrating the processing of the nascent lagging strand of an arrested replication fork at the yeast RFB. (1) Schematic drawing of a progressing replication fork. Only a selection of the proteins involved in DNA replication is depicted. The replicative helicase, moving in 3′-to-5′ direction along the parental leading strand, promotes DNA unwinding at the replication fork. The bulk DNA synthesis is carried out by polδ/PCNA on the leading and, possibly, on the lagging strand. In general, the growing point of the leading strand is ahead of the synthesized nascent lagging strand. The single-stranded stretches on the parental lagging strand are covered with RP-A, an ssDNA-binding protein (not depicted). (2) The replication fork is stalled, possibly by a DNA-binding protein (Fob1p?). The nascent leading stand comes to a stop. At the same time an RNA-DNA primer is synthesized on the single-stranded stretch of the parental lagging strand by the polα/primase complex. Because the helicase moves along the parental leading strand, the primer is synthesized and processed ahead of the growing point of the nascent leading strand. (3) The gap to the penultimate Okazaki fragment is filled. This might be accomplished by the polα/primase complex or, as depicted here, by the polymerase synthesizing the bulk of the lagging strand. (4) Removal of the primers and ligation of the nick on the nascent lagging strand result in an RI where both nascent strands are extended to similar positions.

see reference 2 and 41). As previously shown, a key enzyme of the replication process is the replicative helicase, which operates ahead of the DNA synthesis and promotes the unwinding of the DNA duplex. The yeast replicative helicase has not yet unequivocally identified. However, there is evidence suggesting that a complex of three minichromosome maintenance (MCM) proteins (Mcm4, -6, and -7) functions as a replicative DNA helicase at the yeast replication fork (1, 14). As depicted in Fig. 7, the MCM helicase tracks 3′ to 5′ on the DNA, thus using the parental leading strand as the template strand (14). Upon encountering the RFB from the nonpermissive direction, the replication fork will be arrested, possibly by a DNA-binding protein inhibiting the replicative helicase, similar to what has been proposed for the bacterial replication arrest at the Ter sites (17). The lagging arm will expose a stretch of ssDNA up to the unwinding point, stabilized by an ssDNA-binding-protein (RP-A), whereas the replicative helicase occupies a part of the unwound parental leading strand. As a result, the nascent leading strand will not be extended up to the unwinding point. The polα/primase complex will prime DNA synthesis by synthesizing an iDNA on the lagging template strand, close to the unwinding point and ahead of the 3′ end of the nascent leading strand. Subsequently, the gap to the penultimate Okazaki fragment will be filled, either by the polα/primase complex itself or by the polymerase synthesizing the bulk of the lagging strand, possibly polδ. Finally, the RNA primer and probably the iDNA will be removed with the help of a helicase and nucleases (2, 41). If the last Okazaki fragment is processed by such a mechanism, the lagging strand will be extended to a position ahead of the leading strand. Whether the placement of the 5′ end of the DNA ahead of the 3′ growing end of the nascent leading strand, a salient feature of this model, is a general mechanism of the DNA replication process or a peculiarity of the replication fork block at the RFB remains to be determined. This model would also explain the relatively homogenous placement of the Okazaki fragments giving rise to major signal at position 418.

An alternative model could involve an initial interference with the synthesis of the leading strand only. This could lead to an uncoupling of the lagging strand synthesis similar to that proposed for replication fork bypass of a lesion located on the leading strand (8). The lagging strand would be elongated further until it also would be stalled by some replication fork blocking activity, which could be located at a similar position to that blocking the nascent leading strand. The salient feature of this model is two separable blocking activities for the nascent leading and the nascent lagging strand.

The stalled replication fork, Fob1, and recombination. The overlapping of sequences essential for replication fork blockage at the RFB and HOT1-dependent mitotic recombination suggests a relationship between the two events. This notion was corroborated by the identification of the *FOB1* gene, which is essential for both HOT1 and RFB functions (20). Furthermore, Fob1 has been shown to be essential for the expansion and contraction of the rDNA repeats and plays a role in the generation of extrachromosomal rDNA circles (10, 18). For both processes, a model involving the stalled replication fork as a substrate for a recombination process has been proposed. In this model, nuclease cleavage of an exposed single-stranded region results in a double-strand break and subsequent repair by gene conversion. We have found strikingly little ssDNA exposed by the stalled replication fork. Whether this has any functional significance for the relationship between the replication fork blockage and recombinational events remains to be determined.

A model which provides a mechanistic link between replication arrest and homologous recombination has recently been proposed by Defossez et al. (10). A central intermediate in this model is a DNA structure resembling a Holliday junction (Fig. 6D) generated by the pairing of the two nascent strands. In previous work in our group, replication forks stalled at the RFB, which had been psoralen cross-linked *in vivo*, were analyzed by EM (27). From 152 reinspected electromicrographs of forks stalled at the RFB, only one molecule could be interpreted as a Holliday-like structure. This suggests that the annealed nascent strands, if they do exist in such a structure, are either shorter than the resolution of the EM analysis (about 50 bp [32]) or of such low abundance that they are not detected by EM.

Since the EM analysis did not reveal Holliday-like structures at the replication fork, we must assume that such putative Holliday junctions localized at the elongation point will be branched molecules consisting of a three long arms (ca. 2.2 to 2.4 kb) and one very short arm (less than 100 bp). Such mol-

ecules should migrate close to the position of corresponding RIs from which they would originate. If such a structure was present in the RIs we isolated, we should have detected it by endo VII digestion and subsequent primer extension, because endo VII resolves Holliday junctions (28). Nicks would be introduced 2 to 6 bp 3′ to the junction (33), presumably mainly on the homologous arms (21), that is, on the parental leading and nascent lagging strands (Fig. 6D, top). However, since we found primer extension signals only within a stretch of maximally 11 bp from the branch point of the replication fork (Fig. 6C), the annealed nascent strands must be either only a few base pairs long or not abundant enough to be detected in our assay. We formally cannot exclude that we had lost these structures during the 2D gel isolation of RIs. However, during the gel isolation procedure the RIs were heated to 72°C, which probably tend to promote the annealing of the nascent strands.

ACKNOWLEDGMENTS

We are grateful to B. Kemper for generously providing the endo VII enzyme, and we thank N. Mantei and A. Stasiak for critical reading of the manuscript and U. Suter for continuous motivation.

This work was supported by grants from the Swiss National Science Foundation and by the Swiss Federal Institute of Technology (ETH), Zürich (to J.M.S.).

REFERENCES

1. **Aparicio, O. M., D. M. Weinstein, and S. P. Bell.** 1997. Components and dynamics of DNA replication complexes in S. cerevisiae: redistribution of MCM proteins and Cdc45p during S phase. Cell **91:**59–69.
2. **Bambara, R. A., R. S. Murante, and L. A. Henricksen.** 1997. Enzymes and reactions at the eukaryotic DNA replication fork. J. Biol. Chem. **272:**4647–4650.
3. **Bielinsky, A. K., and S. A. Gerbi.** 1998. Discrete start sites for DNA synthesis in the yeast ARS1 origin. Science **279:**95–98.
4. **Brewer, B. J., and W. L. Fangman.** 1993. Initiation at closely spaced replication origins in a yeast chromosome. Science **262:**1728–1731.
5. **Brewer, B. J., and W. L. Fangman.** 1988. A replication fork barrier at the 3′ end of yeast ribosomal RNA genes. Cell **55:**637–643.
6. **Brewer, B. J., D. Lockshon, and W. L. Fangman.** 1992. The arrest of replication forks in the rDNA of yeast occurs independently of transcription. Cell **71:**267–276.
7. **Burhans, W. C., L. T. Vassilev, J. Wu, J. M. Sogo, F. S. Nallaseth, and M. L. DePamphilis.** 1991. Emetine allows identification of origins of mammalian DNA replication by imbalanced DNA synthesis, not through conservative nucleosome segregation. EMBO J. **10:**4351–4360.
8. **Cordeiro-Stone, M., L. S. Zaritskaya, L. K. Price, and W. K. Kaufmann.** 1997. Replication fork bypass of a pyrimidine dimer blocking leading strand DNA synthesis. J. Biol. Chem. **272:**13945–13954.
9. **Dammann, R., R. Lucchini, T. Koller, and J. M. Sogo.** 1995. Transcription in the yeast rRNA gene locus: distribution of the active gene copies and chromatin structure of their flanking regulatory sequences. Mol. Cell. Biol. **15:**5294–5303.
10. **Defossez, P. A., R. Prusty, M. Kaeberlein, S. J. Lin, P. Ferrigno, P. A. Silver, R. L. Keil, and L. Guarente.** 1999. Elimination of replication block protein Fob1 extends the life span of yeast mother cells. Mol. Cell **3:**447–455.
11. **DePamphilis, M. L., and P. M. Wassarman.** 1980. Replication of eukaryotic chromosomes: a close-up of the replication fork. Annu. Rev. Biochem. **49:**627–666.
12. **Gerber, J. K., E. Gogel, C. Berger, M. Wallisch, F. Muller, I. Grummt, and F. Grummt.** 1997. Termination of mammalian rDNA replication: polar arrest of replication fork movement by transcription termination factor TTF-I. Cell **90:**559–567.
13. **Hernandez, P., L. Martin-Parras, M. L. Martinez-Robles, and J. B. Schvartzman.** 1993. Conserved features in the mode of replication of eukaryotic ribosomal RNA genes. EMBO J. **12:**1475–1485.
14. **Ishimi, Y., Y. Komamura, Z. You, and H. Kimura.** 1998. Biochemical function of mouse minichromosome maintenance 2 protein. J. Biol. Chem. **273:**8369–8375.
15. **Jensch, F., and B. Kemper.** 1986. Endonuclease VII resolves Y-junctions in branched DNA in vitro. EMBO J. **5:**181–189.
16. **Kemper, B.** 1997. Branched DNA resolving enzymes, p. 179–204. *In* J. A. Nickoloff and M. Hoekstra (ed.), DNA damage and repair. Humana Press, Totowa, N.J.
17. **Khatri, G. S., T. MacAllister, P. R. Sista, and D. Bastia.** 1989. The replication terminator protein of E. coli is a DNA sequence-specific contra-helicase. Cell **59:**667–674.
18. **Kobayashi, T., D. J. Heck, M. Nomura, and T. Horiuchi.** 1998. Expansion and contraction of ribosomal DNA repeats in Saccharomyces cerevisiae: requirement of replication fork blocking (Fob1) protein and the role of RNA polymerase I. Genes Dev. **12:**3821–3830.
19. **Kobayashi, T., M. Hidaka, M. Nishizawa, and T. Horiuchi.** 1992. Identification of a site required for DNA replication fork blocking activity in the rRNA gene cluster in Saccharomyces cerevisiae. Mol. Gen. Genet. **233:**355–362.
20. **Kobayashi, T., and T. Horiuchi.** 1996. A yeast gene product, Fob1 protein, required for both replication fork blocking and recombinational hotspot activities. Genes Cells **1:**465–74.
21. **Lilley, D. M., and B. Kemper.** 1984. Cruciform-resolvase interactions in supercoiled DNA. Cell **36:**413–422.
22. **Linskens, M. H., and J. A. Huberman.** 1988. Organization of replication of ribosomal DNA in *Saccharomyces cerevisiae*. Mol. Cell. Biol. **8:**4927–4935.
23. **Little, R. D., T. H. Platt, and C. L. Schildkraut.** 1993. Initiation and termination of DNA replication in human rRNA genes. Mol. Cell. Biol. **13:**6600–6613.
24. **Lopez-Estrano, C., J. B. Schvartzman, D. B. Krimer, and P. Hernandez.** 1998. Co-localization of polar replication fork barriers and rRNA transcription terminators in mouse rDNA. J. Mol. Biol. **277:**249–256.
25. **Lucchini, R., and J. M. Sogo.** 1994. Chromatin structure and transcriptional activity around the replication forks arrested at the 3′ end of the yeast rRNA genes. Mol. Cell. Biol. **14:**318–326.
26. **Lucchini, R., and J. M. Sogo.** 1992. Different chromatin structures along the spacers flanking active and inactive *Xenopus* rRNA genes. Mol. Cell. Biol. **12:**4288–4296.
27. **Lucchini, R., and J. M. Sogo.** 1995. Replication of transcriptionally active chromatin. Nature **374:**276–280.
28. **Mizuuchi, K., B. Kemper, J. Hays, and R. A. Weisberg.** 1982. T4 endonuclease VII cleaves Holliday structures. Cell **29:**357–365.
29. **Nethanel, T., T. Zlotkin, and G. Kaufmann.** 1992. Assembly of simian virus 40 Okazaki pieces from DNA primers is reversibly arrested by ATP depletion. J. Virol. **66:**6634–6640.
30. **Newlon, C. S.** 1996. Mechanisms for completing DNA replication, p. 873–924. *In* M. L. DePamphilis (ed.), DNA replication in eukaryotic cells. Cold Spring Harbor Laboratory Press, Cold Spring Harbor, N.Y.
31. **Newton, C. R., and A. Graham.** 1994. PCR, p. 13. BIOS Scientific Publishers Limited, Oxford, United Kingdom.
32. **Portmann, R., W. Schaffner, and M. Birnstiel.** 1976. Parital denaturation mapping of cloned histone DNA from the sea urchin Psammechinus miliaris. Nature **264:**31–34.
33. **Pottmeyer, S., and B. Kemper.** 1992. T4 endonuclease VII resolves cruciform DNA with nick and counter-nick and its activity is directed by local nucleotide sequence. J. Mol. Biol. **223:**607–615.
34. **Ruven, H. J., C. M. Seelen, P. H. Lohman, L. H. Mullenders, and A. A. van Zeeland.** 1994. Efficient synthesis of 32P-labeled single-stranded DNA probes using linear PCR; application of the method for analysis of strand-specific DNA repair. Mutat. Res. **315:**189–195.
35. **Sambrook, J., E. F. Fritsch, and T. Maniatis.** 1989. Molecular cloning: a laboratory manual, 2nd ed. Cold Spring Harbor Laboratory Press, Cold Spring Harbor, N.Y.
36. **Sanchez, J. A., S. M. Kim, and J. A. Huberman.** 1998. Ribosomal DNA replication in the fission yeast, Schizosaccharomyces pombe. Exp. Cell Res. **238:**220–230.
37. **Sanger, F., S. Nicklen, and A. R. Coulson.** 1977. DNA sequencing with chain-terminating inhibitors. Proc. Natl. Acad. Sci. USA **74:**5463–5467.
38. **Sherman, F., G. R. Fink, and J. B. Hicks (ed.).** 1986. Methods in yeast genetics: a laboratory course manual, p. 163–164. Cold Spring Harbor Laboratory Press, Cold Spring Harbor, N.Y.
39. **Sinclair, D. A., and L. Guarente.** 1997. Extrachromosomal rDNA circles—a cause of aging in yeast. Cell **91:**1033–1042.
40. **Skryabin, K. G., M. A. Eldarov, V. L. Larionov, A. A. Bayev, J. Klootwijk, V. C. de Regt, G. M. Veldman, R. J. Planta, O. I. Georgiev, and A. A. Hadjiolov.** 1984. Structure and function of the nontranscribed spacer regions of yeast rDNA. Nucleic Acids Res. **12:**2955–2968.
41. **Waga, S., and B. Stillman.** 1998. The DNA replication fork in eukaryotic cells. Annu. Rev. Biochem. **67:**721–751.
42. **Walmsley, R. M., L. H. Johnston, D. H. Williamson, and S. G. Oliver.** 1984. Replicon size of yeast ribosomal DNA. Mol. Gen. Genet. **195:**260–266.
43. **Wellinger, R. E., and F. Thoma.** 1997. Nucleosome structure and positioning modulate nucleotide excision repair in the non-transcribed strand of an active gene. EMBO J. **16:**5046–5056.
44. **White, M. F., M. J. Giraud-Panis, J. R. Pohler, and D. M. Lilley.** 1997. Recognition and manipulation of branched DNA structure by junction-resolving enzymes. J. Mol. Biol. **269:**647–664.
45. **Wiesendanger, B., R. Lucchini, T. Koller, and J. M. Sogo.** 1994. Replication fork barriers in the Xenopus rDNA. Nucleic Acids Res. **22:**5038–5046.
46. **Wu, J. R., and D. M. Gilbert.** 1995. Rapid DNA preparation for 2D gel analysis of replication intermediates. Nucleic Acids Res. **23:**3997–3998.